Structural and spectroscopic characterization of Lu_2O_3:Eu nanocrystalline spherical particles

2004 J. Phys.: Condens. Matter 16 6983

(http://iopscience.iop.org/0953-8984/16/39/031)

INSTITUTE OF PHYSICS PUBLISHING JOURNAL OF PHYSICS: CONDENSED MATTER

J. Phys.: Condens. Matter **16** (2004) 6983–6994 PII: S0953-8984(04)78349-6

Structural and spectroscopic characterization of Lu_2O_3:Eu nanocrystalline spherical particles

J Trojan-Piegza[1], E Zych[1,3], D Hreniak[2], W Stręk[2] and L Kępiński[2]

[1] Faculty of Chemistry, University of Wrocław, 14 F Joliot-Curie Street, 50-383 Wrocław, Poland
[2] Institute of Low Temperatures and Structure Research Polish Academy of Sciences, 2 Okólna Street, 50-950 Wrocław2, PO Box 1410, Poland

E-mail: zych@wchuwr.chem.uni.wroc.pl

Received 24 March 2004, in final form 7 July 2004
Published 17 September 2004
Online at stacks.iop.org/JPhysCM/16/6983
doi:10.1088/0953-8984/16/39/031

Abstract

Spherical particles of Lu_2O_3:x% Eu, with x varying from 0% to 10% with respect to Lu, were prepared by precipitating hydroxides with urea at 80 °C and subsequently decomposing these hydroxides to oxides at 650 °C. TEM pictures revealed that the spherical particles were very uniform in size and their diameters were about 130 nm. Each of the particles consisted of crystallites about 20 nm in diameter. Luminescence and excitation spectra contained all the characteristic features of the Eu^{3+} ion. The most intense line in the emission was located around 611 nm. Energy transfer was observed from the Eu^{3+} ions occupying the $S_6(C_{3i})$ centrosymmetric site to the Eu^{3+} located in the non-centrosymmetric position of C_2 symmetry. The decay kinetics were slightly non-exponential, especially for the lowest dopant concentrations. At liquid nitrogen temperature the average decay time for the 0.2% powder was shorter by about 40% compared to the 3–10% materials. At room temperature the average decay time varies only slightly. Rise times were observed for all concentrations at room temperature but only for higher concentrations at liquid nitrogen temperature. This effect is in contrast to that of nanoparticles of Lu_2O_3:Eu prepared using different synthesis procedures.

1. Introduction

Nanostructured luminescent materials based on insulators are probably the least understood phosphors. The literature offers results and analyses, which are confusing, indeed. While some authors enthusiastically report on their findings, convinced that the nanocrystalline materials are more efficient emitters and/or the luminescence is faster than for bulk analogues [1–5],

[3] Author to whom any correspondence should be addressed.

others inform about somewhat opposite findings [6–9]. Clearly, as this field of exploration is still new, we should be extraordinarily cautious to avoid being misled by nature. At present the situation is definitely unclear, and we are far from any deeper understanding. Therefore, it is very important to collect the most thorough and reliable experimental data. Day by day such systematic work will reveal still further details on the physics and chemistry of nanostructured phosphors.

Making nanostructured luminescent materials requires low-temperature procedures. Obviously, at higher temperatures the grain growth is strongly stimulated and particles grow to sizes beyond the nanoregime. The low temperature of synthesis is considered a plus, since energy consumption is greatly reduced and often even the equipment can be less sophisticated than for the fabrication of classic coarse phosphors. However, the low temperature of synthesis can be also a problem in the sense that the final product can contain impurities destructive for its luminescent properties. Most of all the experimenter should pay attention to organic remains and/or OH-residue [10–14], whose harmful influence on the luminescence efficiency can be very profound due to high-energy vibrations associated with them.

A number of procedures for the production of nanocrystalline phosphors have been developed. We can easily find many papers showing successful applications of sol–gel procedure, combustion synthesis, spray pyrolysis, molten-salts procedure, and Pechini process for the fabrication of nanostructured phosphors. In fact each of these techniques is being exploited in various modifications with the hope of getting products of better quality. Besides the particle size, among the phosphor parameters being of great importance are the particles' agglomeration and their shape. It is of great significance that particles do not sinter during the preparation and are left separated. Spherical morphology of such non-agglomerated particles is much preferred. Such a shape allows for the most efficient packing (the lowest volume of interparticle voids) and the surface-to-volume ratio is the smallest, making the surface quenching effects less significant. Indeed, there are reports showing that the fabrication of fully spherical particles is possible [15–18].

We turned our attention to the preparation of nanostructured Lu_2O_3 in an inexpensive and technically easy procedure based on homogeneous precipitation of the metal hydroxide from an aqueous solution of the metal salt with ammonia formed through the decomposition of urea at higher temperature. Urea reacts with water at 80–100 °C as follows:

$$CO(NH_2)_2 + H_2O \rightarrow 2NH_3 + CO_2; \tag{1}$$

NH_3 evolves systematically to the solution and the metal hydroxide precipitates steadily as the pH gradually increases. After separation the hydroxide can be decomposed at higher temperatures to the oxide.

We wish to devote a few words to the nature of our interests, which have also received attention from other groups [19–22]. We are looking for materials whose properties make them attractive for ionizing radiation detection, especially for medical diagnosis. Lutetium oxide indeed offers exceptional efficiency in stopping the incoming x-ray radiation. This is an effect of its high density (9.42 g cm^{-3}) and the high Z-number of Lu (71), which makes up as much as 88% (by weight) of the total. If we could fabricate a really efficient lutetia-based x-ray phosphor it could be an attractive substitute for today's standards either in powder form or as a sintered ceramic. In the latter case there is a possibility to make fully transparent plates of Lu_2O_3, since this is isotropic cubic compound [23, 24]. The sintering process is, however, strongly influenced by the properties of the starting powder, which should be fine and non-agglomerated.

Lu_2O_3 host possesses two crystallographic sites for the metal cation. One of them has C_2 and the other $C_{3i}(S_6)$ symmetry. The former, non-centrosymmetric, site when occupied

by a rare earth (RE) ion makes intraconfigurational electric dipole induced f–f transitions possible [25, 26]. The later, however, which is centrosymmetric, allows only for magnetic dipole induced transitions, which are generally less efficient and longer [26, 27]. For Eu^{3+} in a lutetia host we already showed that for the S_6 site only relatively weak lines due to $^5D_0 \rightarrow {}^7F_1$ transitions can be detected [27, 28]. The most prominent feature is located around 582.5 nm. Fortunately, at higher concentrations of Eu^{3+} there is observed an efficient energy transfer from Eu^{3+} in the $S_6(C_{3i})$ site ($Eu(S_6)$) to Eu^{3+} occupying the C_2 site ($Eu(C_2)$). This makes the undesired emission from $Eu(S_6)$ of only negligible intensity and relatively fast for higher concentrations.

2. Materials and experiments

A series of Lu_2O_3:Eu was prepared with the dopant content being 0%, 0.2%, 1%, 3%, 5%, 7%, 10%, and 13%. In a typical synthesis, 1.5 g of $Lu(NO_3)_3{\cdot}5H_2O$, whose appropriate part was replaced with $Eu(NO_3)_3{\cdot}6H_2O$ according to the required composition, and 10 g of urea, $CO(NH_2)_2$, was dissolved in 100 cm^3 of water. All the ingredients were put in a 400 cm^3 beaker. The solution was heated up to about 80 °C and stirred. One undoped specimen was prepared without stirring. After about 6 h the solution with a white precipitate was cooled down and the sediment was separated with a cup-type centrifuge. Afterwards, the obtained material was dried at 300 °C and heated at various temperatures between 500 and 1000 °C for 6 h.

The thermal analysis was performed in the range of 20–1000 °C under nitrogen atmosphere using a SETSYS 16/18 system manufactured by SETARAM. The heating rate was 10 °C min^{-1}. An ARL inductively coupled plasma (ICP) spectrometer was used for a determination of Eu content in the materials.

X-ray analyses were performed with a DRON-1 diffractometer, using Cu Kα-radiation ($\lambda = 1.5418$ Å) filtered with Ni. The diffractograms were recorded with a step of $2\theta = 0.1°$ for a range of $2\theta = 10°$–$120°$. Additional, more precise measurements with a step of $2\theta = 0.01°$ were performed for a selected line of cubic Lu_2O_3 with $(hkl) = (440)$ in the region of $2\theta = 48°$–$51°$. Scherrer's relation [29], equation (2), was used to estimate the crystallite sizes

$$D = \frac{0.9\lambda}{\cos\theta\sqrt{\beta^2 - \beta_0^2}}, \tag{2}$$

where D is the average crystallite size, λ denotes the x-ray radiation wavelength, β is the full-width at half maximum of a diffraction line located at θ, and β_0 represents the scan aperture of the diffractometer. High resolution transmission electron microscopy (TEM) images and selected area electron diffraction (SAED) patterns were taken with a Philips CM20 Super Twin microscope operating at 200 kV and providing 0.25 nm resolution.

Photoluminescence and excitation spectra were recorded using an SPF 500 spectrofluorimeter equipped with a 300 W Xe-lamp with a sapphire window and an Al-coated parabolic reflector. The emission monochromator was equipped with a 1200 line mm^{-1} ruled grating blazed at 500 nm. The excitation monochromator used a 1200 line mm^{-1} holographic grating optimized for 250–300 nm. Excitation spectra were taken with 0.3 nm resolution, and emission spectra with 0.25 nm resolution, and the former were corrected for the excitation light intensity. Emission spectra were not corrected for the setup characteristics, and the sensitivity of the detection system (PMT-grating) was highest in the range of 400–750 nm. Emission kinetics were measured with a Tektronics 1000 TDS 380 oscilloscope using an excimer laser (308 nm) as the excitation source.

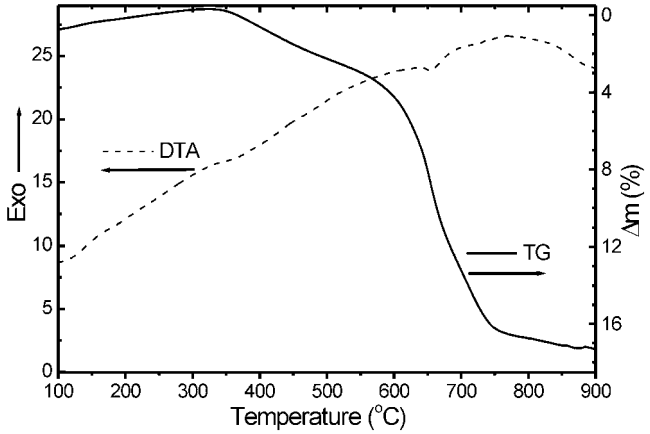

Figure 1. Thermogravimetric analysis of homogeneously precipitated $Lu(OH)_3$ dried at 300 °C.

Table 1. Nominal versus measured (ICP determined) Eu contents in the Lu_2O_3:Eu powders.

Eu concentration (at.%)	
Nominal	ICP measured
1	0.87
3	2.99
5	4.69
7	6.77
10	9.74
13	8.33

3. Results and discussion

About 1 h after starting the preparation process the solution turns slightly opaque, which results from the formation of a precipitate. As the procedure continues the amount of the precipitate increases for the next few hours. We determined that 5–6 h is enough to complete the precipitation process. The white powder separated from the solution and dried was very fine and loose. In table 1 we compare the nominal and the real concentration of Eu in the investigated powders as derived with the ICP technique. These results show that for up to 10% of Eu in the solution, its measured content in the fabricated powder is very close to the nominal content. For the 13% sample the incorporation into the precipitate seems to be hindered. Therefore we decided not to include the results of various measurements for this powder in the paper to avoid any confusion.

In figure 1 we show the results of the thermogravimetric analysis of the raw powders. The obtained pattern is rather straightforward. In the range of 300–600 °C there is observed a gradual loss of the specimen mass, which could be assigned to the loss of one molecule of water per two molecules of $Lu(OH)_3$. Above 600 °C up to about 700 °C there is observed a more significant loss of mass, which can be reliably attributed to the following decomposition:

$$2Lu(OH)_3 \rightarrow Lu_2O_3 + 3H_2O. \tag{3}$$

Thus from the thermogravimetric measurements we can conclude that the raw precipitate is a hydrated lutetium hydroxide, which can be converted into oxide by heating at about 650 °C.

In figure 2 we show x-ray diffraction patterns for specimens heated at specified temperatures between 500 and 1000 °C for 6 h. Figure 2 shows that up to 500 °C the obtained powders are fully amorphous. However, heating at 550 °C for 6 h already stimulates the

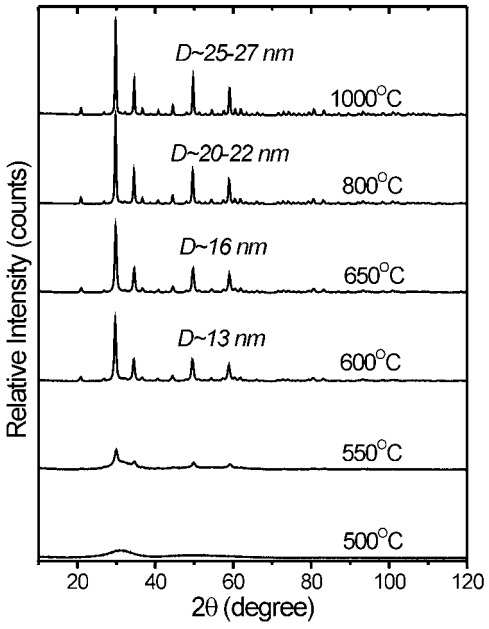

Figure 2. X-ray diffraction patterns of the powders after heating at the indicated temperature for 6 h.

material to crystallization, although the amorphous phase is still clearly seen. Nevertheless, the weak diffraction lines appearing in the pattern are clearly related to Lu_2O_3, which indicates that prolonged heating reduces the $Lu(OH)_3 \rightarrow Lu_2O_3$ decomposition temperature to some extent in comparison with the thermogravimetric analysis. Indeed, the longer exposure of the homogeneously precipitated $Lu(OH)_3$ to a temperature of 600 °C allows the material to fully decompose to crystalline Lu_2O_3. Heating the material at still higher temperatures does not change the total integrated intensity of the diffraction lines, which proves that the crystallization was already complete at 600 °C. However, heating at higher temperatures makes the diffraction lines gradually narrower, which reflects the increasing sizes (D) of the crystallites making up the powder. The numbers are given in figure 2.

In figure 3 we show how the line around $2\theta = 49.6°$ moves towards smaller angles as the concentration of Eu increases. This effect occurs for all diffraction lines. Such behaviour reflects the increasing value of the cubic unit cell parameter, since the Eu^{3+} ion is noticeably larger compared to Lu^{3+} (0.947 versus 0.861 Å) [30]. The variations of the unit cell with Eu content are also shown in figure 3. The diffraction lines in figure 3 are all very symmetrical and we do not see any bumps or any other irregularities on either side of the lines for any concentration of Eu^{3+}. This indicates that even for relatively high Eu contents the dopant seems to be rather uniformly dissolved in the lattice of the host material. Later on this conclusion will get support from spectroscopic measurements.

The TEM images confirm the results of XRD data and reveal additional details. Figure 4 presents images for materials heated at 300 and 650 °C together with a result for the powder prepared without stirring during the precipitation process. First, the beneficial influence of the stirring for the material microstructure is clearly seen. The powder prepared without stirring is far less uniform if the particles sizes are considered. The diameters of the particles varies from about 30 nm to about 200 nm, and their shapes are not regular, although a tendency to form round structures is clearly seen. In contrast, the powder prepared with stirring consists of practically spherical particles which are exceptionally equal in size. Each particle in the

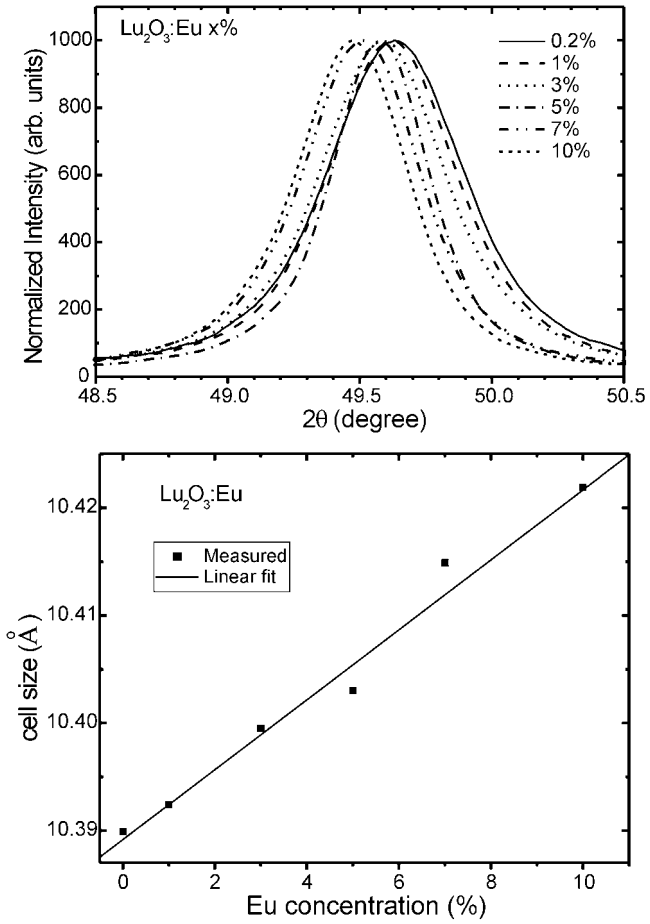

Figure 3. Detailed analysis of the shift of a selected diffraction line $(hkl) = (440)$ with Eu concentration (top) and the derived variation of the unit cell size (bottom).

picture is about 130 nm large. The agglomeration is also only minor. What is more important is that the heating at 650 °C does not stimulate the particles to grow or sinter. They still retain the same size of about 130 nm and have a loose non-agglomerated character. The SAED pattern confirms that the sample treated at 650 °C is crystalline with a cubic structure. HRTEM measurements of the powder heated at 650 °C prove that the crystallites are about 20 nm large, which is close to the value obtained from Scherrer's formula from diffraction line broadening. Thus in the Lu_2O_3:Eu powders obtained at 650 °C each of the spherical particles consists of a number of crystallites of rather similar size.

Figure 5 shows the luminescence spectra under 250 nm excitation for the specimens doped with 1% and 10% of Eu. The measurements were performed at room and liquid nitrogen temperature. The emissions for all specimens differ in overall intensity but in general the luminescence is very similar for various Eu concentrations. Nevertheless, there are some systematic variations in the luminescence. Thus with increasing dopant content the emission lines around 532 nm (see the insets), already weak for the lowest concentration specimen, regularly diminish, and finally at room temperature they practically disappear for specimen of highest concentrations. This emission (532 nm) results from radiative recombination of the $^5D_1$ of the Eu^{3+} ion. As the activator concentration increases the non-radiative energy dissipation down to $^5D_0$ becomes progressively more efficient, and finally the room temperature emission results

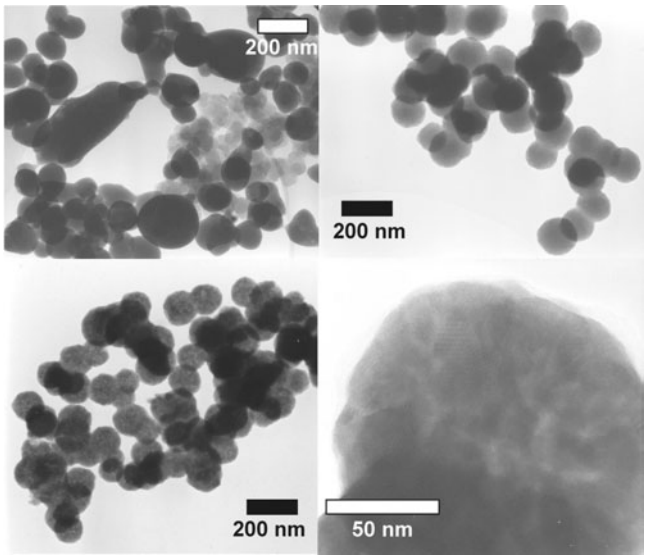

Figure 4. TEM pictures of the various specimens. Top left: $Lu(OH)_3$ precipitated without stirring of the solution; top right: $Lu(OH)_3$ precipitated with continuous stirring of the solution; bottom: Lu_2O_3 formed after heating at 650 °C for 5 h of the $Lu(OH)_3$ precipitated with continuous stirring.

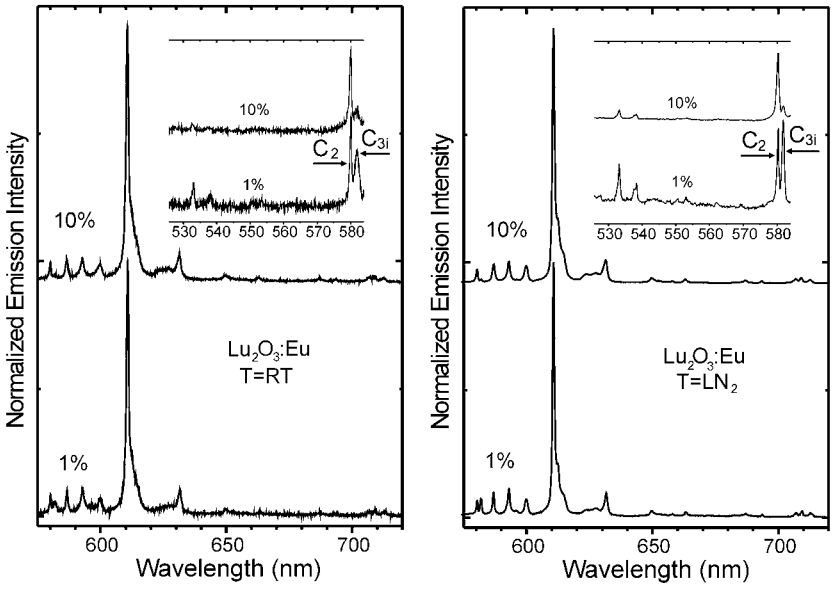

Figure 5. Emission spectra recorded at room (left) and liquid nitrogen (right) temperature for Lu_2O_3:Eu containing 1% and 10% of the dopant. The 582.5 nm line comes from the $^5D_0$–$^7F_1$ emission of the centrosymmetric site $C_{3i}(S_6)$. The line intensity decreases with increasing Eu concentration due to the energy transfer from Eu in the S_6 site to Eu in the C_2 site. The weak emission within the range 530–540 nm (see insets) results from a radiative relaxation of the $^5D_1$ state of Eu^{3+}.

almost exclusively from the $^5D_0 \rightarrow {}^7F_J$ radiative transitions. While generally the same is true for liquid nitrogen temperature, the lines around 532 nm can be easily detected for all investigated concentrations, although their intensities are indeed weak for the highest Eu contents.

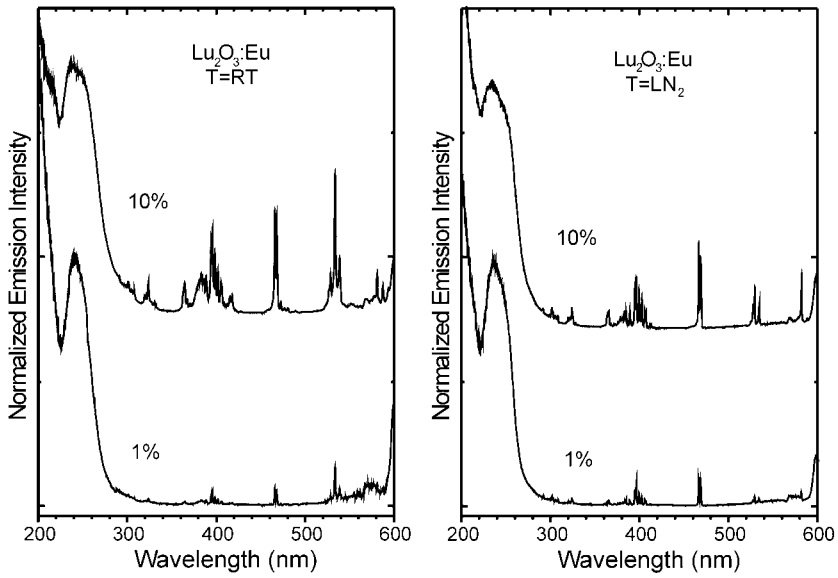

Figure 6. Excitation spectra recorded at room (left) and liquid nitrogen (right) temperature for Lu_2O_3:Eu containing 1% and 10% of the dopant. The narrow lines are due to the intraconfigurational transitions within the 4f levels of Eu^{3+} and the broader band around 250 nm results from the charge-transfer absorption. Compare figure 7.

Around 582.5 nm in the luminescence spectra we see a line, whose intensity also fades with increasing Eu content; see the insets in figure 5. This emission line results from the magnetic dipole induced $^5D_0 \rightarrow {}^7F_1$ radiative recombination of Eu^{3+} occupying the centrosymmetric site S_6. This line intensity gradually diminishes for higher dopant concentrations since the $^5D_0$ level of $Eu(S_6)$ is positioned slightly above the $^5D_0$ of Eu^{3+} in the C_2 site [27, 31]. Once the separation of dopant ions shortens, the probability of $Eu(S_6) \rightarrow Eu(C_2)$ energy transfer obviously increases, and the $Eu(S_6)$ luminescence diminishes.

Figure 6 presents the excitation spectra measured at room and liquid nitrogen temperature for specimens doped with 1% or 10% of Eu. In the spectra we can see an interesting effect scaling the Eu concentration. Namely, the intensity of the intraconfigurational f–f transitions systematically increases compared to the intensity of the CT band with the dopant content. This is not a real effect, however. In figure 7 we present two excitation spectra of the 10% powder recorded with two different procedures. One of the spectra was taken using simply the pure Lu_2O_3:10% Eu powder and the other spectrum was obtained using the same powder mixed in 1:10 mass ratio with undoped Lu_2O_3. The spectrum of the Lu_2O_3:10% Eu powder dispersed in undoped lutetia is practically identical with the spectrum of the 1% specimen already seen in figure 6. A similar situation was described by de Mello Donega *et al* [32, 33], who investigated the concentration dependence of the vibronic transitions probabilities in rare earths. The explanation is then that this is a saturation effect. The absorption of light is so intense in the region of the CT band that in the concentrated systems the light excites practically only a part of the overall depth of the material. The intraconfigurational transitions are much less intense and the light can penetrate much deeper into the material before being completely absorbed. These variations in the absorption efficiencies can easily introduce the artefact effect as we just noted.

In figure 8 we present luminescence decay traces for all the specimens at room and liquid nitrogen temperature. At room temperature each of the decays possesses a characteristic

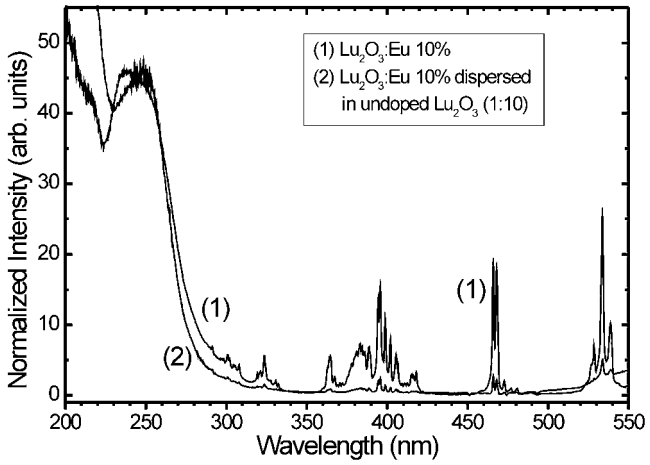

Figure 7. Excitation of Lu_2O_3:Eu 10% recorded for the pure sample and after its dispersion in pure Lu_2O_3. The latter spectrum proves that the variations of the intensities between the CT and f–f transitions seen in figure 6 are artefacts.

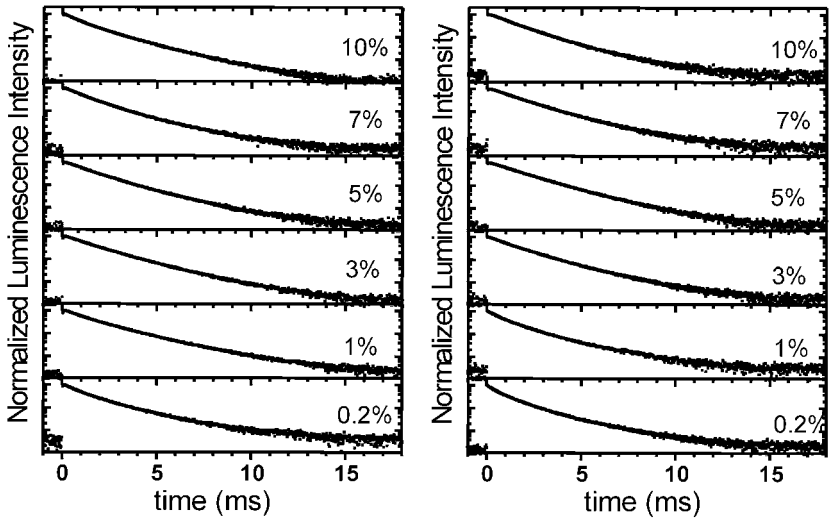

Figure 8. Concentration dependence of the 611 nm emission decay traces at room (left) and liquid nitrogen (right) temperature. All decays are slightly non-exponential.

feature, known as the signal build-up, with its own characteristic time constant, while at liquid nitrogen temperature the rise time is absent for the lowest Eu content. All the decays diverge slightly from single exponential behaviour. Hence, a fitting procedure could be performed with the three-exponential equation

$$I/I_0 = A_1 \exp(-t/\tau_1) + A_2 \exp(-t/\tau_2) + A_3 \exp(-t/\tau_3), \tag{4}$$

where the first of the components having a negative value of A_1 describes the rise time of the decay.

The shape of the decays suggests that they are slightly non-exponential rather than simply two-exponential (forgetting about the rise time). Therefore we calculated the average decay time taking into account the derived values for A_2, A_3, τ_2, and τ_3. While such mathematically derived values do not have any real physical meaning their variations with Eu concentration, see figure 9, are symptomatic. For Eu concentrations of 3–10% the average values of the decay time constants are almost identical for both temperatures. For lower Eu concentrations

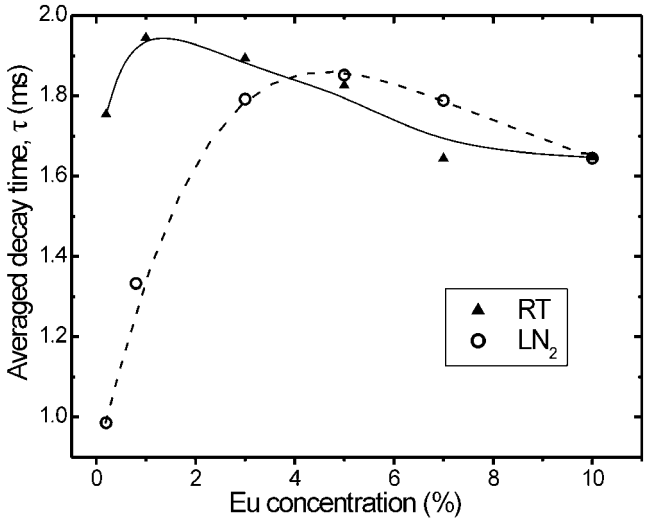

Figure 9. The concentration dependence of the average luminescence decay time at room and liquid nitrogen temperature. Curves drawn to guide the eye.

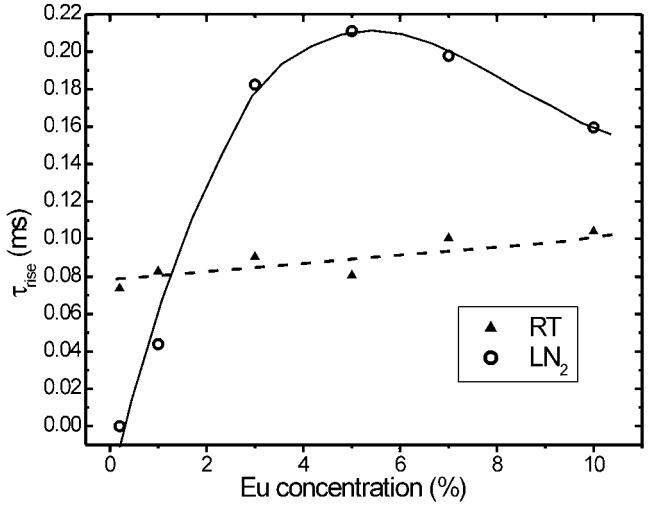

Figure 10. The concentration dependence of the rise time of the 611 nm emission under 308 nm excitation at room and liquid nitrogen temperature. The lines are drawn to guide the eye.

the values at liquid nitrogen temperature drop down, reaching 1 ms for the 0.2% specimen, which is only about 60% of the value for the 5% powder. We shall return to this effect later on. Now we can state that at liquid nitrogen temperature the decay time almost doubles as the Eu concentration increases from 0.2% to 5%.

In figure 10 we show the variations of the rise time with concentration at room and liquid nitrogen temperature. At room temperature the rise time stays almost constant within the whole range of Eu contents. However, at liquid nitrogen temperature the variations are indeed profound. For the lowest concentration of dopant the rise time is totally absent. As the dopant content increases the rise time gets longer, reaching a value of about 0.2 ms for the 5% specimen. At yet higher concentrations the rise time slightly decreases.

Such a behaviour of the rise time with concentration and temperature seems to indicate that both the separation of the Eu^{3+} ions (concentration) and energy of accessible phonons (temperature) are important for the considered property. In general the appearance of a rise time is a result of a slow process of feeding of the emitting level ($^5D_0$). About 1600 cm^{-1}

above the $^5D_0$ state of Eu^{3+} we have the $^5D_1$ level, which is located some 3000 cm^{-1} below the still higher $^5D_2$. The feeding of the emitting state can occur either through a non-radiative multiphonon relaxation from the higher levels or through cross-relaxation. The latter requires rather small separation of the dopant ions *and* a level within the ^7F_J configuration separated from the ground $^7F_0$ state by the same or at least very similar energy as it is for one of the two pairs $^5D_1$–$^5D_0$ or $^5D_2$–$^5D_1$. If there is a mismatch of the two energy gaps an assistance of phonons is required for cross-relaxation to occur [34]. The cross-relaxation is a rather slow process and this could explain the appearance of a rise time at higher concentrations as was observed for Tb^{3+} doped materials [34].

Since at lower temperatures the rise time strongly decreases for lower concentrations, we can conclude that in such conditions the process of non-radiative relaxation down to the emitting $^5D_0$ level is fast. In other words at such conditions the slow non-radiative relaxation process is 'switched off'. As the concentration increases the rise time gets longer. Thus the stronger Eu^{3+}–Eu^{3+} interaction 'switches on' the slow course of a non-radiative relaxation to the $^5D_0$, simultaneously making the fast relaxation path continuously less effective. It was proved [34] that cross-relaxation between Eu^{3+} ions needs not only a reduced separation between them but also the assistance of phonons, since there is some mismatch between the levels involved. It looks as if at the low temperature of liquid nitrogen the separation between Eu^{3+} ions in the most diluted specimen is too large for cross-relaxation to occur. In such a situation the system finds an alternative (fast) path to relax down to the $^5D_0$ level. Thus it seems that the fast and slow non-radiative relaxations down to $^5D_0$ compete all the time, and depending on the temperature and concentration (Eu^{3+} ions separation) one or the other takes the upper hand. At the lower temperature of liquid nitrogen the slow process becomes totally ineffective for the most dilute system, presumably due to the too large separation between the ions.

Once the Eu^{3+}–Eu^{3+} separation is short enough to let the ions interact, cross-relaxation becomes the preferred way of feeding the emitting $^5D_0$ state. Since it requires some phonon assistance, whose accessibility is restricted to some extent at the temperature of liquid nitrogen, the process becomes additionally delayed with decreasing temperature. The experimental results confirm that a fast multiphonon relaxation indeed takes place and is efficient when the Eu–Eu interaction is negligible. As the Eu^{3+} ions start interacting, the energy may migrate between them for some time before the excited electron finally relaxes through cross-relaxation down to the emitting $^5D_0$, from which it can produce its emission. Note that the same effect, the increasing Eu^{3+}–Eu^{3+} interaction, may be responsible for the significant elongation of the low temperature decay time with rising Eu concentration from 0.2% to 5%, as seen in figure 9. Namely, the increasing probability of energy migration and the Eu^{3+}–Eu^{3+} interaction can account for the effectively longer lifetime of the excited electron. Therefore both the temperature and concentration behaviour of the decay time and rise time can be seen as resulting from cooperative interactions between Eu^{3+} ions.

The above considerations, while technically acceptable (although indeed not apparent), become problematic if we compare the results to those obtained by us for other nanocrystalline Lu_2O_3:Eu powders fabricated using different methods [35]. The present phosphor consisting of spherical particles is the only one exhibiting such a pattern of rise time. In all other cases the rise times were always longest for low concentrations independently of temperature, and got shorter with increasing Eu content. This was even true for sintered ceramics with grains of the order of a few microns [35, 36]. Would that imply that this is the *shape* of the particles and/or the arrangement of crystallites within them, which interfere so significantly with the various relaxation processes within Eu^{3+} ions? Now we do not see any alternative explanation but the problem would need a deeper theoretical treatment. It seems to us that this could bring interesting results.

The perfectly spherical shape of our particles implies that they may be very efficiently packed on screens. Such research is in progress and will be reported elsewhere.

Acknowledgment

Financial support from the Polish Committee for Scientific Research (KBN) under grant No 4 T09B 087 23 is gratefully acknowledged.

References

[1] Bhargava R N, Gallagher D, Hong X and Nurmikko A 1996 *Phys. Rev. Lett.* **72** 416
[2] Bhargava R N 1997 *J. Lumin.* **46** 72
[3] Bruchez M Jr, Moronne M, Gin P, Weiss S and Alifisatos A P 1998 *Science* **281** 2013
[4] Sharma P K, Jilavi M H, Nass R and Schmidt H 1999 *J. Lumin.* **82** 187
[5] Li X-Q and Arakawa Y 1999 *Phys. Rev.* B **60** 1915
[6] Efros A L and Rosen M 1997 *Phys. Rev. Lett.* **78** 1110
[7] Chan W C W and Nie S 1998 *Science* **281** 2016
[8] Bol A B and Meijerink A 1998 *Phys. Rev.* B **58** 15997
[9] Bol A B and Meijerink A 2000 *J. Lumin.* **87–89** 315
[10] Ye T, Guiwen Z, Weiping Z and Shangda X 1997 *Mater. Res. Bull.* **32** 502
[11] McKittric J, Shea L E, Sastry I S R and Bacalski C 1998 *Luminescent Materials VI* vol PV97-29, ed C R Ronda and T Welker (San Francisco, CA: Electrochemical Society) p 22 (ISBN 1-56677-182-X)
[12] Zych E 2001 *Opt. Mater.* **16** 445
[13] Zych E, Hreniak D and Strek W 2002 *Mater. Sci.* **20** 111
[14] Yu M, Lin J, Zhou Y H, Wang S B and Zhang H J 2002 *J. Mater. Chem* **12** 86
[15] Tamatani M, Matsuda N, Okumura M, Albessard A K, Inoue Y, Yokota S and Kawasaki K 1998 *Luminescent Materials VI* vol PV97-29, ed C R Ronda and T Welker (San Francisco, CA: Electrochemical Society) p 10 (ISBN 1-56677-182-X)
[16] Flor J, Piers A M, Davolos M R and Jafelicci M Jr 2002 *J. Alloys Compounds* **344** 323–6
[17] Kang Y C, Lenggoro I W, Park S B and Okuyama K 2000 *Mater. Res. Bull.* **35** 789
[18] Očana M 2001 *J. Eur. Ceram. Soc.* **21** 931
[19] Garcia-Murillo A, Le Luyer C, Pedrini C and Mugnier J 2001 *J. Alloys Compounds* **323/324** 74
[20] Weber M J, Derenzo S E, Dujardin C and Moses W W 1996 *Proc. Scint'95* ed P Dorenbos and C W E van Eijk (The Netherlands: Delft University Press) pp 9–16
[21] Derenzo S E, Moses W W, Cahoon J L, Devol T A and Boatner L 1991 *IEEE Nucl. Sci. Symp. Conf. Record* 91CH3100-5 **1** 143
[22] Laversenne L, Guyot Y, Goutaudier C, Cohen-Adad M Th and Boulon G 2001 *Opt. Mater.* **16** 475
[23] *ICSD Collection Code* No. 40471 1990 ed FIZ Karlsruhe & Gmelin Inst. Release 99/1
[24] Lempicki A, Brecher C, Szupryczynski P, Lingertat H, Nagarkar V V, Tipnis S V and Miller S R 2002 *Nucl. Instrum. Methods* A **488** 579
[25] Forest H and Ban G 1969 *J. Electrochem. Soc.* **116** 474
[26] Buijs M, Meijerink A and Blasse G 1987 *J. Lumin.* **37** 9
[27] Zych E 2002 *J. Phys.: Condens. Matter* **14** 5637
[28] Zych E, Karbowiak M, Domagala K and Hubert S 2002 *J. Alloys Compounds* **341** 381
[29] Klug P and Alexander L E 1954 *X-ray Diffraction Procedure* (New York: Wiley) chapter 9
[30] Shannon R D 1976 *Acta Crystallogr.* A **32** 751
[31] Karbowiak M, Zych E and Hölsa J 2003 Crystal field analysis of Eu^{3+} in Lu_2O_3 *J. Phys.: Condens. Matter* **15** 2169–81
[32] de Mello Donega C, Meijerink A and Blasse G 1994 *J. Lumin.* **62** 189
[33] de Mello Donega C 1994 Vibronic spectroscopy of Pr^{3+} in solids *PhD Thesis* Utrecht University, The Netherlands (ISBN 90-393-0813-6)
[34] Blasse G 1988 *Prog. Solid State Chem.* **18** 79–171
[35] Zych E, Hreniak D and Strek W 2002 Spectroscopic properties of Lu_2O_3/Eu^{3+} nanocrystalline powders and sintered ceramics *J. Phys. Chem.* B **106** 3805–12
[36] Strek W, Zych E and Hreniak D 2002 *J. Alloys Compounds* **344** 332–6